Irregular Orbits Generate Higher Harmonics

Gerd van de Sand[1] and Jan M. Rost[1,2]
[1]*Theoretical Quantum Dynamics, Fakultät für Physik, Universität Freiburg, Hermann-Herder-Strasse 3, D-79104 Freiburg, Germany*
[2]*Institute for Advanced Study, Wallotstrasse 19, D-14193 Berlin, Germany and Max-Planck-Institute for Physics of Complex Systems, Nöthnitzer Strasse 38, D-01187 Dresden, Germany*
(Received 25 March 1999)

The spectrum of higher harmonics in atoms calculated with a uniformized semiclassical propagator is presented and it is shown that the higher harmonic generation is an interference phenomenon which can be described semiclassically. This can be concluded from the good agreement with the quantum spectrum. Moreover, the formation of a plateau in the spectrum is specifically due to the interference of irregular, time-delayed, trajectories with regular orbits without a time delay. This is proven by the absence of the plateau in an artificial semiclassical spectrum generated from a sample of trajectories from which the irregular trajectories (only a few percent) have been discarded.

PACS numbers: 32.80.Wr, 03.65.Sq, 05.45.Mt

Higher harmonic generation (HHG) is an intriguing and experimentally well-confirmed phenomenon which results from the nonlinear response of a microscopic system to a strong laser field [1,2]. HHG has been studied in simple but illustrative models numerically and analytically [3–6]; for reviews see [7,8]. Thereby, two striking features have been identified, namely, the occurrence of a "plateau," i.e., the almost constant intensity of the harmonics over a wide range of orders N, and the sharp "cutoff" at a certain maximum order $N_{\max}$ of harmonics. These features have been explained in terms of a simple quasiclassical argument [4,5].

A closer inspection, however, reveals that only the cutoff can be explained with this argument that involves a phase matching condition for the semiclassical amplitude imposing constraints on the actions of representative classical orbits. In the case of an initially bound electron one obtains the intuitively appealing picture that the electron must return to the nucleus in a certain time correlated with the period (frequency) of the laser field to generate higher harmonics [4]. If the electron has too much energy (which it would need to generate extremely high harmonics) it is too fast to fulfill the matching condition. Hence, the matching condition does explain the cutoff, or more precisely, it predicts that the conditions for HHG are unfavorable for $N > N_{\max}$. On the other hand, this does not explain the existence and origin of the plateau for $N < N_{\max}$ since the cutoff condition does not provide a reason why the probability for HHG should be (almost uniformly) high for $N < N_{\max}$ as it is found in experiments and in numerical simulations. Indeed, only in quantum simulations is the plateau found; classical simulations do not yield a plateau. This raises the question whether the plateau is due to inherently quantum mechanical effects, such as diffraction or tunneling, or if it is a pure interference phenomenon that can be explained semiclassically.

In order to answer this question one must carry out a full semiclassical calculation of HHG which has not been done so far. This is probably due to considerable technical difficulties since the chaotic dynamics of the explicitly time dependent problem renders a standard semiclassical treatment (even for 1 spatial degree of freedom) in the framework of the van Vleck propagator [9] impossible. However, using a uniformized propagator following the ideas of Hermann and Kluk [10,11] we have succeeded in obtaining a converged semiclassical spectrum of HHG. Moreover, we are able (i) to prove that HHG is a pure interference effect, and (ii) to identify the different types of trajectories which interfere with each other.

We have performed our calculation with the "canonical" model system for the interaction of a strong laser field with a one-electron atom, described by the Hamiltonian,

$$H = p^2/2 + V(x) + E_0 x \cos\omega t\,, \tag{1}$$

where $V(x) = -(x^2 + a^2)^{-1/2}$ with $a^2 = 2$ is the so-called "soft core" potential (atomic units are used if not stated otherwise). With this choice of a the ground state energy in the potential V corresponds to that of hydrogen, $E = -1/2$ a.u. The other parameters which will be used are $E_0 = 0.1$ a.u. and $\omega = 0.0378$ a.u. We propagate a wave packet $\Psi(x,t)$ according to

$$|\Psi(x,t)\rangle = U(t)\,|\Psi(x,0)\rangle\,. \tag{2}$$

The initial wave packet has its center $x_0 = E_0/\omega_0^2 = 70$ atomic units away from the nucleus (located at $x = 0$) and is defined as

$$\Psi(x,0) = \left(\frac{\gamma^2}{\pi}\right)^{1/4} \exp\left(-\frac{\gamma^2}{2}\,\Delta_{xx_0}^2 + \frac{i}{\hbar}\,p_0\Delta_{xx_0}\right), \tag{3}$$

with $\Delta_{ab} = a - b$, $\gamma = 0.2236$ a.u., and $p_0 = 0$ a.u. Under these conditions of a scattering experiment the cutoff for HHG occurs at $2U_p = (E_0/\omega)^2/2$; see also [6]

 0031-9007/99/83(3)/524(4)$15.00

where the same initial conditions have been used. Only the width γ was chosen differently in [6]; however the cutoff does not depend on γ.

The Gaussian form of $\psi(x,0)$ allows one to express the semiclassically propagated wave function in closed form as an integral over phase space [11],

$$\Psi(x,t) = \frac{1}{(2\pi\hbar)} \int\int dq\, dp\, R_\gamma(p_t,q_t) \exp\left(\frac{i}{\hbar} S(p_t,q_t)\right) \exp\left(-\frac{\gamma^2}{2}\Delta^2_{xq_t} + \frac{i}{\hbar} p_t \Delta_{xq_t}\right) \times \exp\left(-\frac{\gamma^2}{4}\Delta^2_{qx_0} - \frac{1}{4\gamma^2}\Delta^2_{pp_0} + \frac{i}{2\hbar}\Delta_{qx_0}(p + p_0)\right), \quad (4)$$

where $S(p_t,q_t)$ is the classical action of a trajectory at t, and

$$R_\gamma(p_t,q_t) = \left| \frac{1}{2}\left(M_{qq} + M_{pp} - i\gamma^2\hbar M_{qp} - \frac{1}{i\gamma^2\hbar} M_{pq}\right)\right|^{1/2} \quad (5)$$

is composed of all four blocks $M_{ab} = \partial^2 S/(\partial a \partial b)$ of the monodromy matrix.

From the time dependent wave function we construct the dipole acceleration,

$$d(t) = -\left\langle \Psi(t) \left| \frac{dV(x)}{dx} \right| \Psi(t) \right\rangle, \quad (6)$$

from which the harmonic spectrum

$$\sigma(\omega) = \int d(t) e^{i\omega t}\, dt \quad (7)$$

is obtained by Fourier transform. Typically 10^6 trajectories are necessary to converge $d(t)$ from Eq. (6). For comparison we have also determined $d(t)$ quantum mechanically (Fig. 4) using standard fast Fourier transform split operator methods to compute the wave function $\Psi(x,t)$.

Figure 1 demonstrates that a plateau and a cutoff are visible in the quantum (a), and in the semiclassical (c) harmonic spectrum, but not in the classical (b) one. Since the semiclassical spectrum (c) and the quantum spectrum (a) are very similar we may conclude that HHG can be described semiclassically. (Small differences at the absolute level of $\sigma \approx 10^{-6}$ a.u. beyond the cutoff frequency can be attributed to the limited numerical accuracy of the semiclassical propagation.) Furthermore, the absence of the plateau in the classical spectrum (b) suggests that it is due to an interference effect of different types of classical trajectories contributing to the semiclassical result (c).

Among the classical trajectories from which the semiclassical dipole acceleration Eq. (6) is constructed we can distinguish trajectories which suffer a time delay when passing the nucleus (i.e., $x \approx 0$) from the "mainstream" trajectories which are not slowed down. Furthermore, among the time-delayed trajectories we can identify two groups.

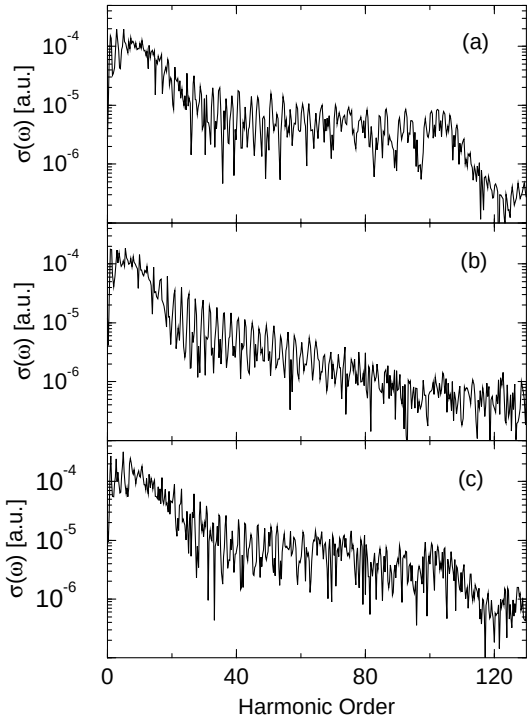

FIG. 1. Quantum (a), classical (b), and semiclassical (c) spectrum of higher harmonics according to Eq. (7).

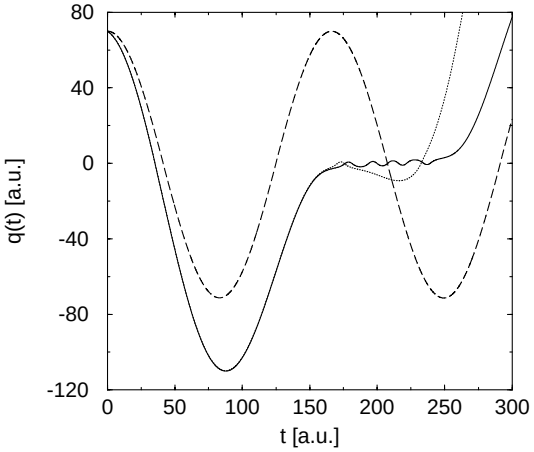

FIG. 2. Examples for direct (dashed line), stranded (dotted line), and trapped (solid line) trajectories; see text.

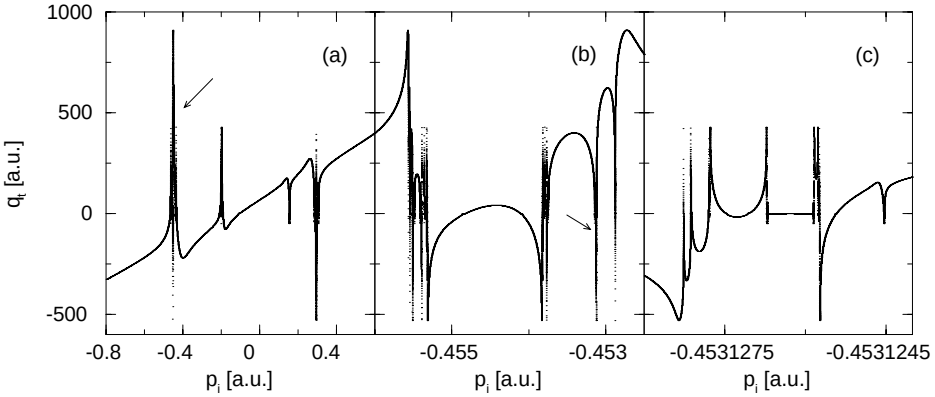

FIG. 3. Deflection function $q_t(p_i)$ for $t = 3T$ and $x_i = x_0 = 70$ a.u. demonstrating the chaotic character of the trapped trajectories. The arrows indicate the range of the next higher enlargement.

Trajectories of the first group (dotted line in Fig. 2) get "stranded" on top of the barrier of the effective potential $V_{\text{eff}}(x) = V(x) - E_0 x$. The second group is formed by trajectories which become temporally "trapped," (solid line in Fig. 2). The trapped trajectories are chaotic in the sense of an extreme sensitivity to a change in initial conditions. This is clearly seen in the deflection function $q_t(p_i)$ (Fig. 3) where the final position q_t of a trajectory at fixed time t is plotted versus its initial momentum p_i [12].

One sees that in certain intervals of p_i small changes in p_i lead to a completely different q_t with the result that the deflection function exhibits a fractal structure. The fractal initial conditions (for a fixed final q_t) belong to those trajectories which are trapped in the potential for a certain dwell time (the solid lines in Fig. 2).

The time-delayed irregular orbits are responsible for the higher harmonics since their contributions interfere with those from the mainstream trajectories. The interference manifests itself in a dephasing in the dipole response $d(t)$ of Eq. (6) after the first encounter with the nucleus (roughly after the time $t = T \equiv 2\pi/\omega$ for our initial conditions) as can be seen in Fig. 4(b). At this time the peak at about $p_i \approx -0.45$ a.u., emerges in the deflection function; see Fig. 3. This corresponds to the return of the nucleus in the case of an initially bound electron as discussed, e.g., in [4,5]. The rich structure of this peak emerges for longer times (see Fig. 3) necessary to resolve the fractal dynamics on a fine scale of the initial conditions p_i. The dephasing in $d(t)$ is clearly an interference phenomenon since it does not occur in the classical dipole response (Fig. 4a).

Having identified the orbits, or equivalently, the initial conditions, which are responsible for the higher harmonics we can artificially construct a harmonic spectrum without those contributions to double check that they are really responsible for HHG. This has been done in the semiclassical spectrum of Fig. 5b where the time-delayed trajectories (about 3% of all initial conditions) have been discarded. Clearly, the plateau has disappeared and the spectrum is similar to the purely classical spectrum with trajectories for all initial conditions included (Fig. 1b). Discarding only the trapped trajectories (0.6%) smears out the cutoff and leaves a reduced plateau for lower harmonics (Fig. 5a). Hence, the quantitative semiclassical reproduction of the quantum HHG spectrum together with the absence of higher harmonics in the classical case (Fig. 1) *and* in the semiclassical case if irregular, time-delayed trajectories are discarded (Fig. 5) confirms our explanation of the origin of the higher harmonics.

To summarize we have shown that higher harmonic generation can be interpreted as a semiclassical interference effect between regular and time-delayed trajectories of the electron. The time delay is either due to a temporal trapping which generates chaotic dynamics or due to a stranding on top of the potential barrier. Along with this time delay goes a characteristic difference in action compared

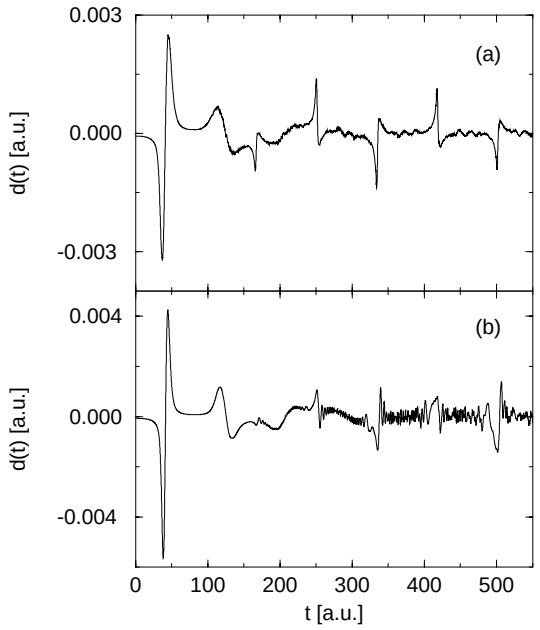

FIG. 4. Classical (a) and semiclassical (b) dipole acceleration according to Eq. (6).

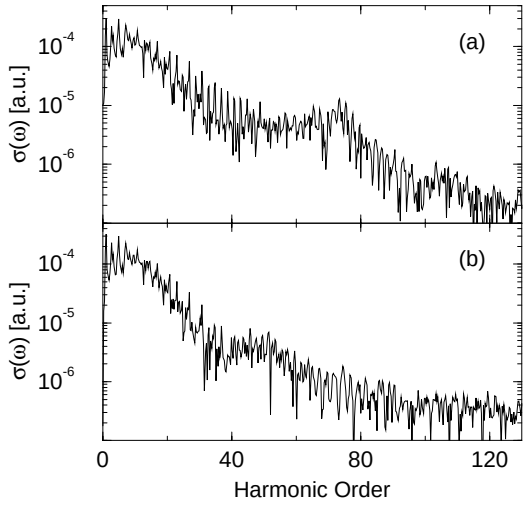

FIG. 5. Semiclassical HHG spectrum as in Fig. 1 but without trapped trajectories (a), and without time-delayed trajectories (b); see text.

to the undelayed mainstream orbits. Analytical quasiclassical approximations of various kinds have been used to derive this phase difference which can explain the cutoff [4,5]. However, as demonstrated here, the full semiclassical expression is far more complicated since for the HHG spectrum chaotic trajectories exhibiting a fractal deflection function are essential. The chaotic character of the irregular orbits allows them to have a relative large effect in comparison to their weight among all initial conditions (of the order of 1%) because their instability leads to a dramatic increase of their weight R_γ in Eq. (5) in the course of time. This increase makes an accurate semiclassical computation rather difficult. Remarkably, despite the chaotic dynamics of the trapped trajectories, one can obtain a converged semiclassical spectrum if a proper semiclassical propagator such as the Hermann-Kluk propagator is used which does not break down at the (abundantly occurring) caustics. The resulting semiclassical harmonic spectrum agrees well with the quantum spectrum.

We would like to thank O. Frank for the calculation of the quantum spectrum and C. H. Keitel for helpful discussions. Financial support from the DFG under the Gerhard Hess-Programm and the SFB 276 is gratefully acknowledged.

[1] A. L'Huillier, L.-A. Lompre, G. Mainfray, and C. Manus, Adv. At. Mol. Phys. Suppl. **1**, 139 (1992).
[2] J. J. Macklin, J. D. Kmetec, and C. L. Gordon III, Phys. Rev. Lett. **70**, 766 (1993); A. L'Huillier and P. Balcou, *ibid.* **70**, 774 (1993).
[3] J. L. Krause, K. J. Schafer, and K. C. Kulander, Phys. Rev. Lett. **68**, 3535 (1992).
[4] P. B. Corkum, Phys. Rev. Lett. **71**, 1994 (1993).
[5] M. Lewenstein, P. Balcou, M. Y. Ivanov, A. L'Huillier, and P. B. Corkum, Phys. Rev. A **49**, 2117 (1994).
[6] M. Protopapas, D. G. Lappas, C. H. Keitel, and P. L. Knight, Phys. Rev. A **53**, R2933 (1995).
[7] K. C. Kulander, K. J. Schafer, and J. L. Krause, Adv. At. Mol. Phys. Suppl. **1**, 247 (1992).
[8] M. Protopapas, C. H. Keitel, and P. L. Knight, Rep. Prog. Phys. **60**, 389 (1997).
[9] J. H. van Vleck, Philos. Mag. **44**, 842 (1922).
[10] M. F. Herman and E. Kluk, Chem. Phys. **91**, 27 (1984).
[11] K. G. Kay, J. Chem. Phys. **100**, 4377 (1994).
[12] In general, the deflection function contains important dynamical information about the classical collision process, see, e.g., H. Goldstein, *Classical Mechanics* (Addison-Weseley, Reading, 1980); J. M. Rost, Phys. Rep. **297**, 271 (1998).